ELSEVIER

Thermochimica Acta 390 (2002) 103–111

thermochimica acta

www.elsevier.com/locate/tca

Mechanism of interaction of pyrite with hematite as simulation of slagging and fireside tube wastage in coal combustion

M.C. Mayoral*, M.T. Izquierdo, J.M. Andrés, B. Rubio

Instituto de Carboquímica, CSIC, María de Luna, n. 12, 50015 Zaragoza, Spain

Received 5 February 2002; accepted 13 February 2002

Abstract

Iron-bearing minerals have been recognised as a mayor source of fire-side wall slagging in pulverised fuel boilers, which not only reduces the thermal efficiency of heat transfer of the exchangers surface, but also affects its integrity as a result of corrosion and erosion. Nevertheless, the root cause of adhesion and growing of deposits has not been clearly addressed. Our approach suggests that differential scanning calorimetry (DSC) combined with simultaneous thermogravimetry can follow the chemical reaction between pyrite and the outer layer of iron oxide on tubewalls. The changes in composition are followed by X-ray diffraction (XRD). The results indicated that the mechanism of wetting and adherence of molten pyrite over iron oxides is chemically induced: both di and mono iron sulphides interact with the oxide layer, changing the oxidation state of iron in oxide scale, from hematite to magnetite. This would imply a change in the protective ability of the scale as well as a great increment in corrosion tendency.

Keywords: Slagging; Fireside corrosion; Pyrite; Iron oxides

1. Introduction

Iron-bearing minerals have been recognised as a mayor source of wall slagging. It is well-known that the deposition of molten or semi-fused particles of pyrite residues may have a significant role in the initial stages of slagging [1,2]. Slagging not only reduces the thermal efficiency of heat transfer at the exchanger surface, but also affects its integrity as a result of corrosion and erosion. In fact, molten salt or slag-related attack is considered as one of the main causes of corrosion of the water wall: the local disruption of the normal oxide film on the tubewalls by intrusion of molten slag can lead to accelerated oxidation or (if sulphur species are present in the slag) to oxidation–sulphidation [3]. A great public and private effort has been invested in describing the extent and reduction of waterwall wastage due to ash deposits when special burner configurations are used (air-staged low NO_x combustion, for instance) [4,5]. Research on slagging has been focused on finding indices or parameters that might predict the decomposition tendency for a certain coal or coal blends in real and simulated combustion environments [6]. Advanced prediction schemes based on computer-controlled scanning electron microscopy (CCSEM) fly ash data and computational fluid dynamics (CFD) are developed to study the slagging propensity of coals [7].

Nevertheless, the root cause of adhesion and growth of deposits has not been clearly addressed, and in fact,

* Corresponding author. Tel.: +34-976-73-3977; fax: +34-976-73-3318.
E-mail address: mayoral@carbon.icb.csic.es (M.C. Mayoral).

0040-6031/02/$ – see front matter
PII: S0040-6031(02)00075-8

all computational approaches to the problem would need as input a chemical description of the system. The present work is focused on the study of the chemical interactions of molten iron species impacting onto metallic tube banks. The background of the problem is well-known: pyrite plays a major role in slagging due to the formation of low melting FeS–FeO intermediates (eutectic point at 940 °C) and the fluxing effect of FeO in aluminosilicates [8,9]. Molten transformed pyrite particles wet oxidised metal surfaces and adhere to the metal during impact. The adherence has been explained in terms of changes in physical characteristics like changes in surface tension, state of the surface, porosity [10,11]. Nowadays, the evolution of the oxide scales is studied as a function of temperature and erodent agents in pilot plants [12] and the morphology of surfaces exposed and metal loss rates [13]. There are fewer examples of fundamental work describing slag formation and deposition mechanisms [14,15]. Our approach proposes that, to test whether the actual bonding mechanism is chemical as opposed to physical, differential scanning calorimetry (DSC) combined with simultaneous thermogravimetry can follow the chemical reaction between pyrite and iron oxide. Calorimetry has been found to be very useful in describing deposition and fluxing phenomena in slagging conditions [16], and thermogravimetry has been used to measure the corrosion behaviour of SS316 in different atmospheres [17]. The changes in composition are followed by XRD, a very useful technique in this field [18].

2. Experimental

2.1. Materials

Natural pyrite (FeS_2) was sieved to $\phi < 40$ μm and stored under inert atmosphere.

Hematite (Fe_2O_3) was prepared by calcination of iron sulphate ($FeSO_4{\cdot}7H_2O$, reagent grade, from Merck) in a muffle furnace at 800 °C for 2 h. The formation of Fe_2O_3 was confirmed by the weight loss and by XRD.

Iron monosulphide (FeS) or pyrrhotite was prepared by heating pyrite to 700 °C in Ar atmosphere, and keeping that temperature for 30 min. FeS formation was confirmed by the weight loss and by XRD.

Test coupons of hematite and its mixtures were prepared by press pelletising in an IR press to ensure close contact of components.

2.2. DSC

The TA SDT 2960 allows simultaneous registry of weight loss and heat flow along thermal treatment of samples. Samples were laid onto the tared Pt pans and heat treatments consisted of a heating ramp of 80 °C min^{-1} to the desired temperature. For most of the experiments, the final temperature was 1350 °C. For several of the experiments, heating was stopped after the main thermodynamic phenomena, i.e. after pyrite decomposition (800 °C) and after first fusion peak (1100 °C). An inert atmosphere was maintained by a constant flow of 90 ml min^{-1} Ar. The determination of enthalpy changes as the integration of the area under the corresponding peak, at the studied conditions, has an estimated experimental error of 1.73%.

2.3. X-ray diffraction (XRD)

The phase constitution of the iron species was investigated with XRD analysis using a Siemens D500 diffractometer set to select Cu Kα radiation. The diffraction angle scanned was 20–70° 2θ using a step size of 0.05° 2θ.

3. Results

3.1. Pyrite decomposition

The decomposition of pyrite with temperature is followed in DSC by the weight change and the endothermic peak. It is shown in Fig. 1. DTGA curve is shown as well in the figure. The decomposition reaction is as follows:

$$FeS_2 \rightarrow Fe_{1-x}S + \tfrac{1}{2}S_2 \quad (1)$$

The area and maximum of the peak would depend on the heating rate like decomposition loss of one sulphur atom to form pyrrhotite ($Fe_{1-x}S$) starts at 500 °C and ends at 750 °C when heated at 80 °C min^{-1}. The observed enthalpy change for the decomposition is $\Delta H = 905.6$ J/g FeS_2, close to the expected value of $\Delta H = 916.67$ J/g FeS_2 [19]. When the particle

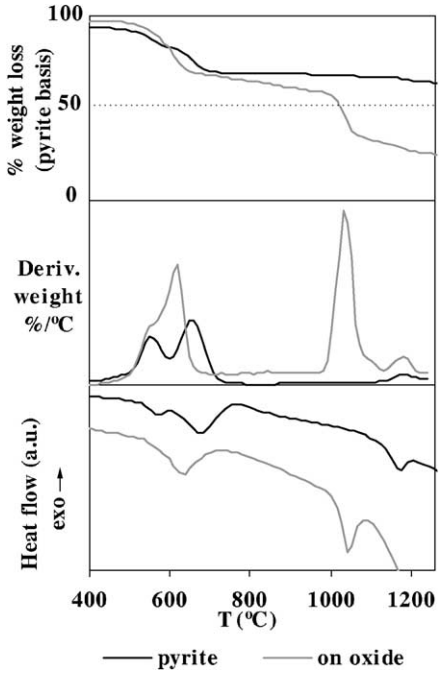

Fig. 1. Weight loss (in pyrite basis), DGTA curves and heat flow profiles of thermal decomposition of pyrite and pyrite laid on an hematite disc.

temperature attains the melting point of pyrrhotite, the particle begins to form a liquid phase. Pyrrhotite fusion appears as an endothermic peak at 1150 °C, with a slight weight loss, probably due to a higher tendency of molten sulphide to oxidise. Even in pure Ar atmosphere, residual traces of oxygen can diffuse to the particle surface to form magnetite, which dissolves in the melt, to form an iron oxysulphide melt. The enthalpy of fusion is 256.02 J/g FeS_2, close to the expected value. These results confirm the calibration and adjustment of the technique and experimental procedure for this calorimetric study.

3.2. Pyrite onto hematite discs

The external surface of water wall tubes is considered to be an oxide scale of Fe_2O_3 (hematite). To test the chemical interaction of pyrite with the hematite, DSC experiments were run for pyrite deposited onto hematite discs, the mass loss, DTGA curve and heat flow profiles of pyrite decomposition are displayed in Fig. 1. It is clearly seen that the final mass loss of pyrite onto hematite is developed in two steps. Firstly, till 700 °C, the pyrite onto hematite decomposes in the same extent as pure pyrite, although the shape of heat flow peak is different. The weight loss line has a decreasing tendency till 1000 °C, when fusion is supposed to start, where there is another big decrease in weight which is accompanied by a big endothermic phenomena.

The mass balance indicates that at 700 °C, the pyrite onto hematite has lost the weight equivalent to the decomposition of the disulphide into monosulphide. XRD (Fig. 2) was unable to detect pyrrhotite in these samples. A previous work has mentioned the difficulties in detecting pyrrhotite by XRD in iron-sulphide containing slagging deposits [20]. The main chemical interaction happens at 1100 °C, when the monosulphide melts, and the mass loss is higher than that corresponding to the release of the sulphur from the monosulphide. The diffractogram obtained for a sample heated to 1100° indicates the presence of a certain proportion of magnetite, and it is even higher for the sample at 1350 °C (Fig. 2). Blank experiments with hematite thermally treated at the same experimental conditions followed by XRD indicated no change in composition, so the transformation into magnetite observed in the sample should be due to a chemical interaction. To adjust the mass balance, the transformation of hematite to magnetite could be taken into account, following the reaction:

$$3Fe_2O_3 \rightarrow 2Fe_3O_4 + \tfrac{1}{2}O_2 \quad (2)$$

This possibility would imply the interaction of pyrite with iron reduction, and the mechanism is studied in Section 3.3.

3.3. Pyrite and hematite

Mixtures of pyrite with hematite at different proportions were studied in DSC. The weight loss in pyrite weight basis, DGTA curves and heat flow profiles are shown in Fig. 3. Sample a is pure pyrite. Sample b is a pellet of pyrite with 50% hematite. For both samples, the decomposition of pyrite losing one sulphur is confirmed by the mass lost at 700 °C, but the shape of the curves is different when mixed with oxide, the pyrite seems to decompose in one step and at lower temperature. This fact is confirmed by the shape of the endothermic decomposition peak.

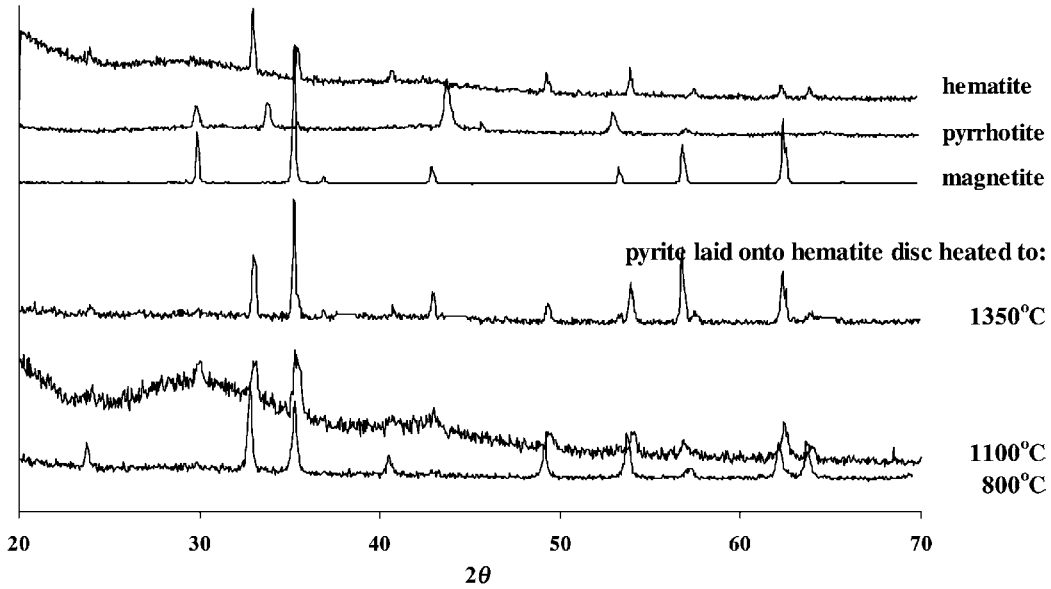

Fig. 2. XRD of pure hematite, pyrrhotite and magnetite, and the diffractograms obtained for pyrite laid onto an hematite disc heated to 800, 1100 and 1350 °C.

The enthalpy change of decomposition for sample b (Table 1) is lower than the enthalpy for pure pyrite, which indicates that decomposition is more favourable when mixed with hematite. Once pyrite decomposed, the evolution of the iron monosulphide is different at higher temperatures when mixed with oxide, another mass loss step is detected starting at 1000 °C. At the same temperature, a big endothermic peak seems to indicate that a fusion phenomenon has taken part simultaneously with the mass loss (areas in Table 1). Several tests were performed over the sample b obtained after heat treatment of 50% mixture. XRD identified pyrrhotite, but surprisingly, the hematite was not detected by XRD. Instead, clear peaks of magnetite indicate the transformation of the oxide into a minor oxidation state, i.e. chemical reduction.

Elemental analysis of the treated mixture b indicated that the percentage of sulphur remaining in the sample agrees with the decomposition of pyrite into pyrrhotite loosing one sulphur per iron atom. So, the second step in mass loss at 1000 °C can not be due to the release of more sulphur, and the mass loss at 1000 °C is in agreement with the release of oxygen in oxide reduction following Eq. (2). In this way, two chemical interactions are detected in mixtures of pyrite with hematite: decomposition of pyrite occurs

Table 1
Enthalpy changes for the decomposition at low temperature (500–700 °C) and fusion and decomposition high temperature (1000–1100 °C)

Sample	Composition	Enthalpy change (J/g pyrite)		T_{onset} fusion (°C)
		Decomposition	Fusion	
a	Pyrite	905	256	1137
b	50% Pyrite	660	415	991
c	33% Pyrite	748	293	986
d	17% Pyrite	1073	114	986
e	8% Pyrite	1498	–	–

Experimental error: 1.73%.

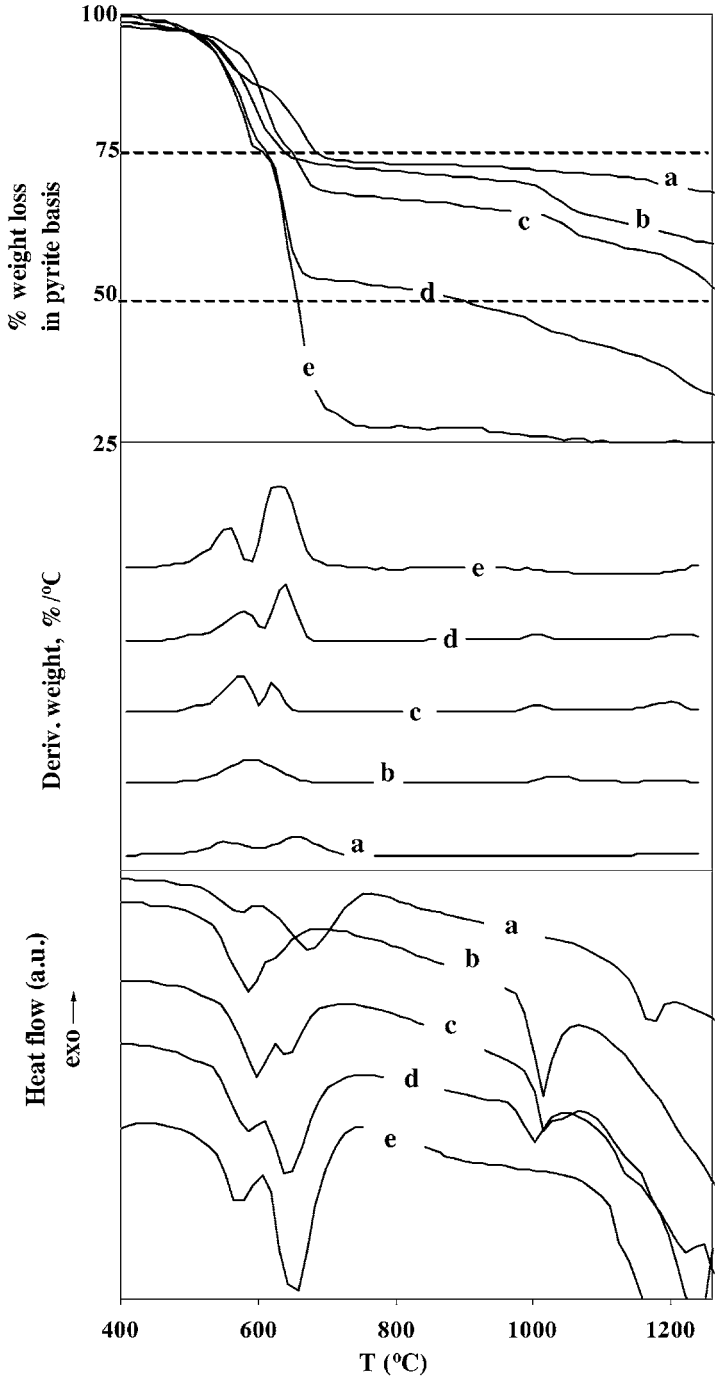

Fig. 3. Weight loss in pyrite weight basis, DGTA curves and heat flow profiles of thermal evolution of pyrite and its mixtures with hematite. a: pure pyrite; b: 50% pyrite; c: 33% pyrite; d: 17% pyrite; e: 8% pyrite.

at lower temperature, and an interaction of hematite with the molten iron monosulphide develops into a chemical reaction of oxide reduction.

3.4. Pyrite and hematite at higher proportions of hematite

Decreasing the proportion of pyrite in the mixture, sample c was prepared with 33% pyrite/64% hematite, and sample d with 17% pyrite/83% hematite. The weight loss of these mixtures (Fig. 3), is in the range of 500°–700 °C, in two steps. Firstly, the disulphide losses one sulphur to form the monosulphide, as expected, but DTGA lines show a sharper peak than for mixture b. The second weight loss step, starting a 630 °C, is detected as well by the heat flow line, as another endothermic decomposition peak. Peak areas in J/g of pyrite are shown in Table 1. The fusion peak appears at the same temperature for samples b, c and d, decreasing the area when the proportion of hematite increases. Fusion areas are shown as well in the table.

Taking into account that the weight loss lines are in initial pyrite weight basis, it is clearly seen in Fig. 3 that the weight loss in mixtures increases as hematite content does. The weight loss is higher than that expected with the release of one sulphur of the disulphide and the oxygen of the conversion of hematite into magnetite. To test the evolution with the temperature, XRD characterisation of the mixture d heated to 800, 1100 and 1350 °C were performed, as well as the elemental analysis of the three samples.

The XRD shown in Fig. 4, indicate that the hematite has almost disappeared at 800 °C, transformed into magnetite. This transformation is complete at 1100 °C. At 1350 °C, there is a peak at 42 2θ that is compatible with the presence of wustite (FeO).

On the other hand, the elemental analysis indicate that the sulphur content at 800 °C implies the total transformation of the disulphide into monosulphide, and part of the monosulphide into elemental iron. The release of sulphur increases with temperature, but there is still a slight amount of sulphur in the sample d at 1350 °C.

The mechanism we propose is that the iron disulphide interacts with the hematite following the equation:

$$FeS_2 + 6Fe_2O_3 \rightarrow Fe + 2SO + 4Fe_3O_4 \quad (3)$$

In this way, the stoichiometric proportion by weight is 11.1% pyrite over hematite. Following this equation, the mass balance of mass loss in samples c (33% in pyrite) and d (17% in pyrite) is fully justified by stoichiometric pyrite interacts with the hematite, which losses the oxygen to form magnetite. Excess pyrite just decomposes into the monosulphide pyrrhotite. This mechanism justifies as well the lack of

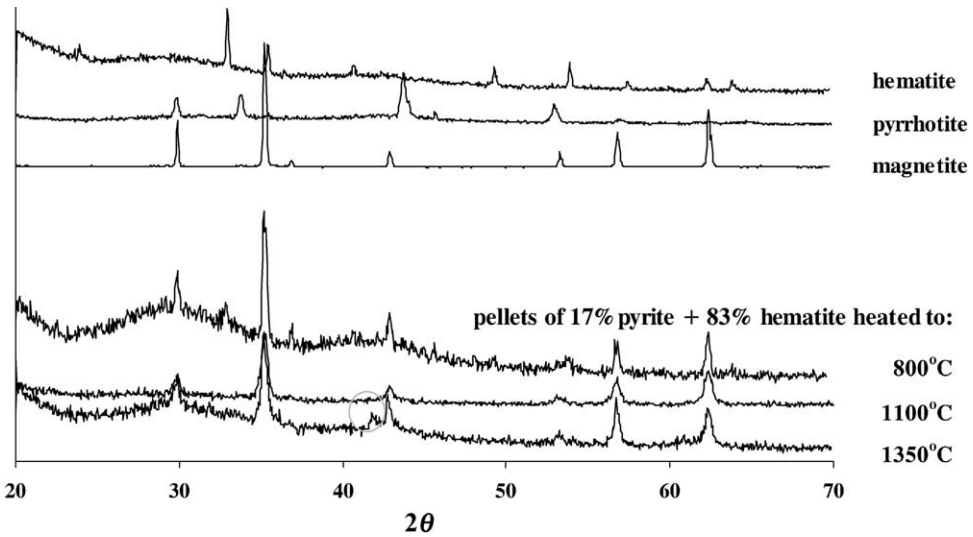

Fig. 4. XRD of pure hematite, pyrrhotite and magnetite, and the diffractograms obtained for sample d heated to 800, 1100 and 1350 °C.

pyrrhotite detection in XRD. On the other hand, the peak at 42 2θ, although, it is present in magnetite diffractogram, could account as well of the present of elemental iron.

The proposed Eq. (3) justifies, as explained above, the mass balance and the XRD characterisation for samples a, b, c and d. To prove the proposed mechanism, a mixture with excess of hematite was prepared, 8% in pyrite, sample e. The mass loss and heat flow profiles are shown in the Fig. 3. It is possible to see that the mass loss corresponds to a first step of pyrite decomposition, similar to previous experiments, and a big change in weight that fits accurately what expected form the Eq. (3) like loss of sulphur from disulphide to elemental iron, and loss of the oxygen from the stoichiometric hematite. XRD of sample e at 1350 °C confirmed the presence of hematite, and the total loss of sulphur was ratified by elemental analysis.

Apart from mass balance and chemical characterisation of final sample, there is another way to test the proposed mechanism. Since the starting supposition is that the first endothermic peak is the sum of two decompositions, pyrite and hematite, the areas of those peaks should be proportional to the mass involved. All the values based in the initial weight of pyrite, the equation should be as follows:

$$\Delta H_{\text{total}}(\text{pyrite}) = H_{\text{dec. of pyrite}}(\text{pyrite}) + H_{\text{dec. of hematite}}(\text{hematite}) \times W \quad (4)$$

where

$$W = \frac{\text{g hematite in initial mixture}}{\text{g pyrite in initial mixture}}$$

or

$$W^* = \frac{\text{g hematite converted after Eq. (3)}}{\text{g pyrite in initial mixture}}$$

From experiments c and d, where pyrite was in excess, we took ΔH_{total} and W (Table 2) and in this way the heats of decomposition were calculated: $H_{\text{dec. of pyrite}} = 516.5$ J/g pyrite and $H_{\text{dec. of hematite}} = 114$ J/g hematite. With these values, it is possible to calculate the variation in enthalpy for both W and W^* (Table 2). In this way, Table 2 shows how the value calculated for experiment e, with excess hematite, fits the experimental value with W^*. These calculations corroborate the validity of the proposed mechanism.

3.5. Pyrrhotite and hematite

The monosulphide obtained by heating pyrrhotite to 700 °C for 30 min, was mixed with hematite and pressed as pellets. In Fig. 5, it is possible to see how pyrrhotite decomposes and losses weight when in contact with excess iron oxide (88%). That weight loss, in pyrrhotite basis, is higher than that corresponding to the loss of the sulphur (this would be a 40% by weight).

If pyrrhotite would react with the oxide following the equation:

$$\text{FeS} + 3\text{Fe}_2\text{O}_3 \rightarrow \text{Fe} + \text{SO} + 2\text{Fe}_3\text{O}_4 \quad (5)$$

The weight loss in pyrrhotite basis would be a 54% considering the loss of the sulphur and the stoichiometric oxygen from the oxide. It is clear from Fig. 5 that this mass is lost when pyrrhotite is mixed with the hematite. Moreover, elemental analysis of the resulting solid at 1350 °C shows that the final content

Table 2
Experimental and calculated variation of enthalpy for the endothermic peak at 500–700 °C as a function of the amount of initial and reacted hematite weight

Sample	Composition	W	W^*	ΔH (J/g pyrite)		
				Experimental	Calculated	
					With W	With W^*
b	50% Pyrite	1	1	660	630	630
c	33% Pyrite	2.03	2.03	748	748	748
d	17% Pyrite	4.88	4.88	1073	1073	1073
e	8% Pyrite	11.9	8.01	1498	1873	1430

Experimental error: 1.73%.

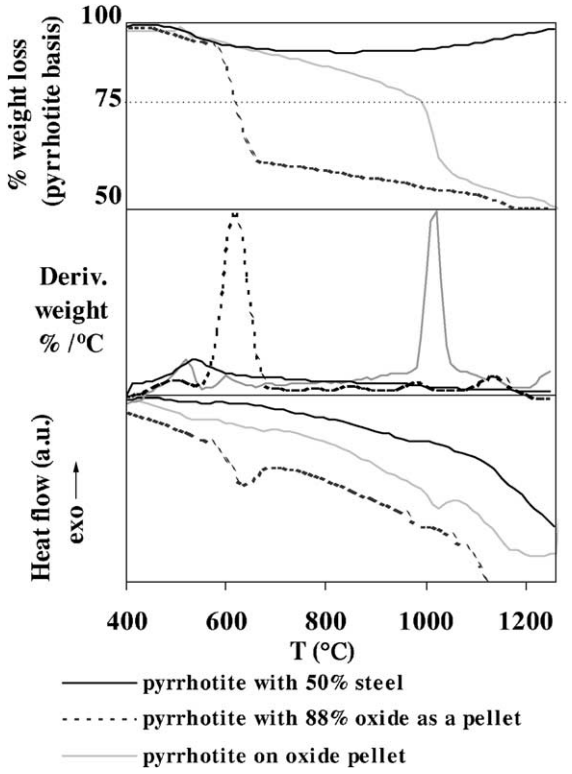

Fig. 5. Weight loss (in pyrrhotite basis), DGTA curves and heat flow profiles of thermal decomposition of pyrrhotite, pyrrhotite with 88% hematite as a pellet, and pyrrhotite laid on an hematite disc.

of sulphur is 0. When pyrrhotite is let to interact on an hematite disk, the evolution is similar to that presented by pyrite (Fig. 1) like low degree of contact implies that the monosulphide must be in a molten state to interact with the oxide and decompose into elemental iron and hematite into magnetite.

4. Conclusions

The results shown in this work indicate that the iron monosulphide has chemical interaction with iron oxides depending on the degree of contact between both species. For the experiments where pyrite were laid onto oxide discs, DSC showed that iron sulphide is able to reduce Fe_2O_3 into Fe_3O_4 following Eq. (3) at high temperatures (1000–1100 °C). Moreover, if high degree of contact is achieved by pelletising mixtures of pyrite with hematite, the proposed mechanism occurs between 600 and 700 °C. Provided that water wall temperature in coal burners is considered to be between 500 and 700 °C, a chemical interaction between the iron sulphide and the iron oxide scale can occur if the contact is high. The kinetic models used for the interpretation of excluded pyrite transformation inside coal burners propose that the particles which impact in tube banks are low viscosity melted FeS droplets. Even for oxidising conditions, the particle impacting is a melted droplet of the eutectic FeS–FeO [21]. In this way, the particles adhere on a deep impact in a liquid state, reaching a high degree of contact with the exposed surface. All the findings discussed above imply that the mechanism of wetting and adherence of molten pyrite over the outer surface of tube banks, is not only physically but chemically induced by iron monosulphide interacts with the Fe_2O_3 oxide layer, and by changing the oxidation state of iron. This would imply a change in the protective ability of the scale as well as a great increment in corrosion tendency. Another important conclusion is that the DSC has shown to be an interesting technique to monitor the chemical interactions between the different surfaces with the ash constituents.

References

[1] E. Raask, Mineral Impurities in Coal Combustion, Behaviour Problems and Remedial Measures, Hemisphere Publishing, Bristol, PA, 1985.
[2] G.P. Huffman, F.E. Huggins, A.A. Levasseur, O. Chow, S. Srinivasachar, A.K. Mehta, Fuel 68 (1989) 485.
[3] I.G. Wright, ASM Metals Handbook, Vol. 13 (Corrosion), ASM International, Materials Park, OH, 1992.
[4] W.T. Bakker, S.C. Kung, Mat. Comp. (DoE and EPRI) 145 (2000) 1.
[5] S. Kihara, K. Nkagawa, I. Kajigaya, Corros. Its Control, Proc. Int. Conf. Corros. 1 (1997) 99.
[6] A.R. McLennan, G.W. Bryant, C.W. Bailey, B.R. Stanmore, T.F. Wall, Energy Fuels 14 (2000) 349.
[7] F.C.C. Lee, F.C. Lockwood, Prog. Energy Comb. Sci. 25 (1999) 117.
[8] S.J. Groves, J. Williamson, A. Sanyal, Fuel 66 (1987) 461.
[9] A.R. McLennan, G.W. Bryant, B.R. Stanmore, T.F. Wall, Energy Fuels 14 (2000) 150.
[10] A.K. Moza, L.G. Austin, Fuel 60 (1981) 1057.
[11] M.F. Abbott, A.K. Moza, L.G. Austin, Fuel 60 (1981) 1065.
[12] Y. Tsumita, K. Namba, I. Kajigaya, K. Sonoya, in: Proceedings of the 14th International Conference on Fluid,

Bed Combustion, Edition 921, Vol. 2, American Society of Mechanical Engineers, 1997.
[13] S.R.J. Saunders, D.D. Gohil, S. Osgerby, Mater. High Temp. 14 (1997) 237.
[14] H.M. ten Brink, J. Eenkhoorn, G. Hamburg, Fuel 78 (1996) 952.
[15] H.B. Vuthaluru, S. Eenkhoorn, G. Hamburg, P.G.T. Heere, J.H.A. Kiel, Fuel Proc. Tech. 56 (1998) 21.
[16] M.C. Mayoral, M.T. Izquierdo, J.A. Andrés, B. Rubio, Themochim. Acta 373 (2001) 173.
[17] S. Frangini, Oxid. Met. 53 (2000) 139.
[18] P.C.J. Graat, H.W. Zandbergen, M.A.J. Somers, E.J. Mittemeijer, Oxid. Met. 53 (2000) 221.
[19] S. Srinivasachar, A.A. Boni, Fuel 68 (1989) 829.
[20] K. Laursen, F.J. Frandsen, Fuel Proc. Tech. 58 (1998) 45.
[21] H.M. ten Brink, J. Eenkhoorn, G. Hamburg, Fuel 78 (1996) 945.